SYNTHESIS, GROWTH, AND CHARACTERIZATION OF MALACHITE GREEN DYE-DOPED POTASH ALUM: STRUCTURAL, OPTICAL, THERMAL, AND NONLINEAR OPTICAL STUDIES FOR OPTOELECTRONIC APPLICATIONS

Shrikant Yadav[1], M. I. Baig[2]

[1] Department of Physics, Prof. Ram Meghe College of Engineering and Management, Badnera, Amravati, 444701, Maharashtra, India

[1] Department of Physics, Yashwantrao Chavan College of Science Karad, Vidyanagar, Karad, 415124, Maharashtra, India.

[2] Department of Physics, Prof. Ram Meghe College of Engineering and Management, Badnera, Amravati, 444701, Maharashtra, India

shrikantyadav17@gmail.com   mirza.baig@prmceam.ac.in

Abstract

This study presents the first successful growth of malachite green-doped potash alum (MG-PAS) single crystals using the slow evaporation technique at ambient conditions. Structural characterization via PXRD confirmed the retention of the cubic Pa-3 space group, with peak sharpening indicating improved crystallinity in the doped samples. FT-IR spectroscopy verified MG incorporation through distinct vibrational shifts, revealing host-guest interactions. UV-Vis analysis showed a reduced band gap in MG-PAS, although optical transmission decreased due to dopant absorption. Thermal analysis revealed an increase in stability during the initial dehydration and intermediate decomposition stages, attributed to hydrogen bonding and electrostatic interactions between MG and the PAS matrix. However, the phase transition temperature slightly decreased in doped crystals, while the final decomposition temperature increased from 970°C (pure PAS) to 991°C (MG-PAS), indicating partial lattice stabilization. Z-scan measurements demonstrated enhanced nonlinear optical properties, with third-order susceptibility (χ^3) increasing from 3.1335×10^{-7} esu to 4.0338×10^{-7} esu, along with an increase in the nonlinear refractive index (n_2) and absorption coefficient (β). These findings establish MG-PAS as a promising candidate for nonlinear optical applications, with improvements in thermal stability during early decomposition stages, despite trade-offs in phase transition behavior and optical transparency.

Keywords: PXRD, FTIR, Optical properties, Thermal Properties, Z-scan.

Introduction

Potassium aluminum sulfate dodecahydrate (PAS), commonly known as potash alum ($KAl(SO_4)_2 \cdot 12H_2O$), is a widely studied inorganic material with applications spanning water purification, pharmaceuticals, food processing, and leather tanning [1-6], Beyond its conventional uses, PAS has gained increasing attention in the field of crystal growth and nonlinear optics (NLO) due to its exceptional transparency in the ultraviolet-visible (UV-Vis) range, high solubility, and well-defined crystallization behavior. It belongs to the family of

sulfate-based crystals, which are known for their diverse structural configurations and tunable electronic properties, making them potential candidates for photonic and optoelectronic applications[7,8].

Structurally, PAS crystallizes in the cubic system, with its dodecahydrate form exhibiting a robust hydrogen bonding network. This extensive hydration not only stabilizes the lattice but also influences its dielectric and optical characteristics. The presence of sulfate groups within the framework allows for modifications in electronic distribution, which can be further manipulated through doping strategies[9,10]. Literature shows that the nonlinear optical (NLO) properties of centrosymmetric crystals can be enhanced by incorporating dopants, which induce structural distortions and break inversion symmetry, leading to improved optical responses [11-13]. Organic dye doping has emerged as a promising approach, as organic molecules possess highly delocalized π-electron systems, which contribute significantly to polarizability, charge transfer interactions, and enhanced nonlinear optical behavior[14-17]. By introducing suitable dye molecules into the PAS lattice, it is possible to alter its electronic structure, induce local asymmetry, and improve optical performance, making the material viable for photonic applications such as laser frequency conversion, optical switching, and optical limiting.

Malachite green (MG) is a cationic triphenylmethane dye known for its strong absorption in the visible region and excellent nonlinear optical properties[18,19]. It has the chemical formula $C_{23}H_{25}N_2Cl$. Its extensive conjugated π-electron system enables significant charge delocalization, resulting in enhanced third-order NLO effects such as nonlinear absorption and refraction. The incorporation of MG into PAS is expected to influence crystal growth kinetics, modify lattice parameters, and introduce defect states that facilitate improved optical and dielectric properties. Malachite green dye's interaction with sulfate and aluminum ions in PAS may lead to localized charge redistribution, thereby further enhancing the material's nonlinear response.

To the best of our knowledge, this is the first study to explore the effect of Malachite Green doping in potash alum and its influence on structural, optical, thermal, and nonlinear optical properties.

Characterisation Studies

The grown pure and methyl orange (MO)-doped potassium aluminum sulfate (potash alum) crystals were subjected to various characterization techniques to evaluate their structural, spectral, optical, thermal, and nonlinear optical (NLO) properties. To confirm the phase purity and crystallinity of the grown crystals, powder X-ray diffraction (PXRD) analysis was carried out using a Bruker Advance D8 diffractometer, scanning over a 2θ range of 10° to 90° with a step size of 0.08°. To study molecular vibrations and confirm the presence of functional groups, Fourier-transform infrared (FTIR) spectroscopy was performed in ATR mode using a Thermo Nicolet 380 FTIR spectrophotometer within the 400–4000 cm⁻¹ range at room temperature. Optical transparency and electronic transitions of the grown crystals were analyzed using UV-Vis absorption spectroscopy, carried out on a

Systronics Double Beam UV-Vis Spectrophotometer in the wavelength range of 190–1100 nm.

To assess the thermal stability, thermogravimetric analysis (TGA) and differential thermal analysis (DTA) were conducted using a Perkin-Elmer Diamond TG-DTA instrument under a nitrogen atmosphere. The nonlinear optical (NLO) properties of the grown crystals were analyzed using the Z-scan technique with a continuous-wave He-Ne laser (632.8 nm) having a beam diameter of 5 mm and a peak intensity of 14.25 kW/m². The transmittance was recorded at a finite aperture in the far field while the sample was moved along the z-axis, allowing the measurement of third-order nonlinear optical responses such as optical limiting and multi-photon absorption.

Material Synthesis and Single crystal growth:

High-quality single crystals of pure potassium aluminum sulfate dodecahydrate (PAS) were successfully grown using the slow evaporation solution growth technique. Merck-grade $KAl(SO_4)_2 \cdot 12H_2O$ was dissolved in double-distilled water to prepare a saturated solution. The solution was continuously stirred at room temperature until complete dissolution was achieved. To ensure purity, it was filtered using Whatman filter paper and placed in a temperature-controlled bath, where it was left undisturbed to undergo slow evaporation under controlled conditions. After five days, spontaneous nucleation occurred, leading to the formation of high-quality seed crystals. A well-developed, transparent seed crystal was carefully selected and suspended in the supersaturated solution to facilitate uniform growth. Within 12 days, a colorless, transparent single crystal of PAS with dimensions of $15 \times 15 \times 10$ mm³ was successfully obtained.

For the synthesis of MG-doped PAS crystals, 1 mol Malachite Green (MG) was introduced into the saturated PAS solution. The growth conditions remained identical to those used for pure PAS crystals. The presence of MG influenced the crystallization process, extending the growth period. Doped crystals began forming within 10 days, and after 22 days, a well-developed MG-doped PAS crystal with dimensions of $11 \times 11 \times 5$ mm³ was obtained. The doped crystal exhibited a distinct coloration, confirming successful dye incorporation while maintaining structural integrity, transparency, and well-defined edges. Figures 1(a) and 1(b) depict the as-grown pure and MG-doped PAS crystals, respectively.
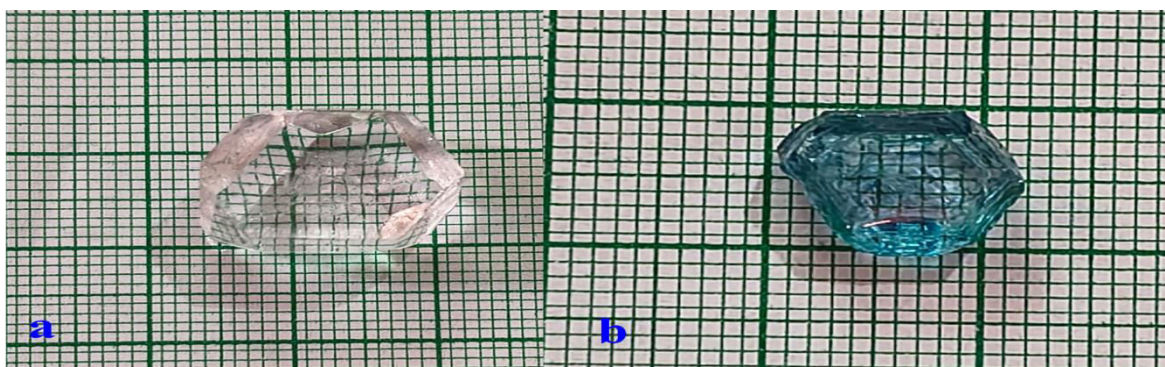

Fig. 1. a) Single Crystal Pure PAS b) MG-PAS

Results and Discussion

Powder X-ray diffraction (PXRD) studies

Powder X-ray diffraction (PXRD) analysis was conducted to examine the structural modifications induced by Malachite Green (MG) doping in potassium aluminum sulfate dodecahydrate (PAS). The diffraction patterns of pure PAS were analyzed and compared with reference data from the Crystallography Open Database (COD) entry no. 1011177, confirming phase purity and structural integrity. Using GSAS-II software, the crystallographic parameters of pure and MG-doped PAS (MG-PAS) were refined, revealing subtle variations caused by dye incorporation. The PXRD patterns for both samples are displayed in Figure 2.
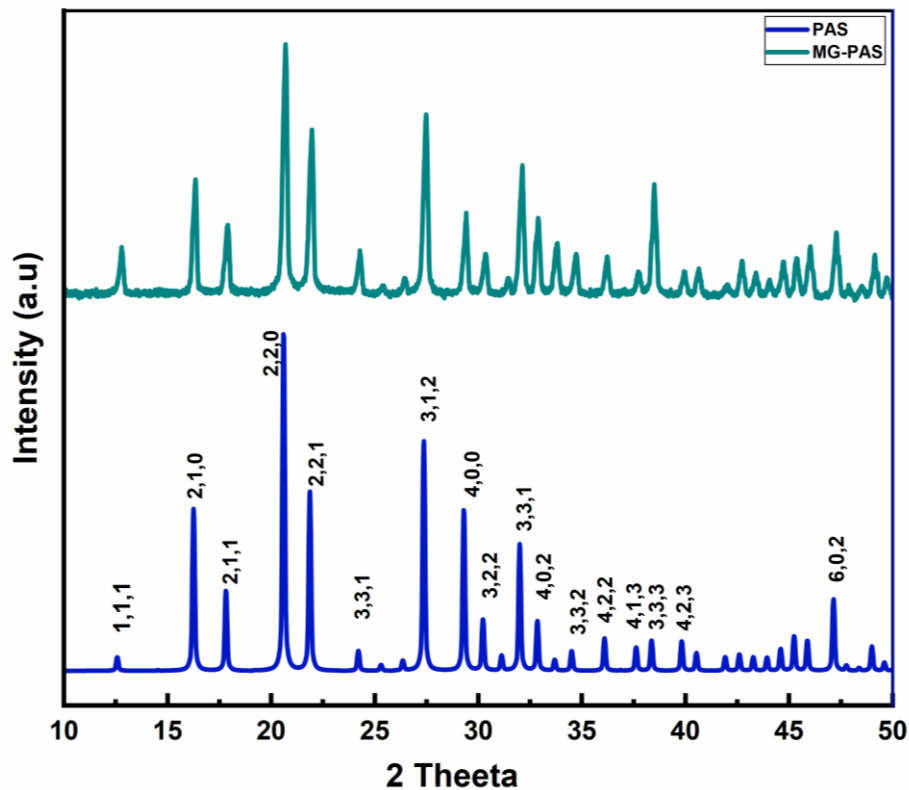

Fig. 2. X-ray powder diffraction patterns of as-grown pure and MG-doped PAS single crystals.

The diffraction peaks in pure PAS were sharp and well-defined, indicating excellent crystallinity with minimal internal strain. In contrast, MG-PAS exhibited minor peak shifts and broadening, suggesting lattice distortions induced by the presence of MG molecules

within the PAS matrix. These shifts may result from local strain and slight unit cell expansion, as the dye molecules interact with the PAS framework.

The full width at half maximum (FWHM) values remained low in both cases, confirming that the crystal quality was well-preserved despite doping. However, the subtle peak distortions in MG-PAS indicate a modification in crystal packing, which could influence its optical and electronic behavior. The successful integration of MG within the PAS lattice without disrupting its fundamental cubic structure suggests that dye doping has introduced localized electronic effects rather than a complete structural transformation.

A comparative summary of the crystallographic parameters for pure and MG-PAS is provided in Table 1.

Table no.1 Lattice parameters of Pure and MG-doped Potash alum.

Crystal data	PAS (Reported Work) PWXRD) [20]	PAS (Present work PWXRD)	PAS (From COD) ID: 1011177	MG-PAS (Present work PWXRD)
a (Å)	12.15	12.19	12.18	12.22
b (Å)	12.15	12.19	12.18	12.22
c (Å)	12.15	12.19	12.18	12.22
α	90	90	90	90
β	90	90	90	90
γ	90	90	90	90
Volume (Å^3)	1793.6	1813	1806.9	1823
System	Cubic	Cubic	Cubic	Cubic
Space group	Pa3	Pa3	Pa3	Pa3

Structural analysis of pure and MG-doped PAS crystals indicated slight variations in lattice parameters, likely resulting from the incorporation of MG molecules into the crystal framework. These subtle changes imply a minor expansion or distortion of the unit cell while retaining the inherent Pa-3 symmetry of the parent crystal structure.

FT-IR spectral analysis

The FTIR spectra of pure PAS and malachite green-doped PAS (MG-PAS) are presented in Figure 3, recorded in the range of 400–4000 cm^{-1} to analyze the vibrational modes of different functional groups. In the spectrum of pure PAS, a broad peak at 3355 cm^{-1} corresponds to the O–H stretching vibration of water molecules present in the crystal lattice. The absorption peak at 2454 cm^{-1} is associated with hydrogen bonding interactions within the PAS structure. A sharp peak observed at 1622 cm^{-1} is attributed to the H–O–H bending vibration from water molecules. The characteristic symmetric and asymmetric stretching vibrations of the sulfate (SO_4^{2-}) group are observed at 1401 cm^{-1}, 1186 cm^{-1}, and 1084 cm^{-1}, confirming the presence of sulfate anions in PAS. Furthermore, peaks at 917 cm^{-1}, 693 cm^{-1}, and 596 cm^{-1} correspond to Al–O stretching vibrations, essential for maintaining the PAS crystal structure.
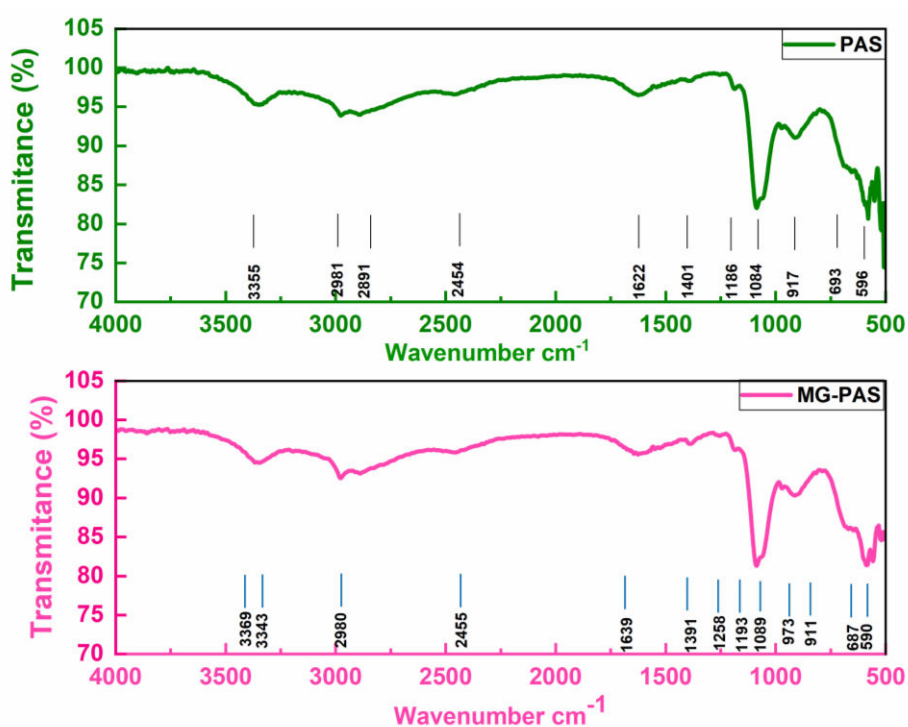
Fig. 3 FTIR spectrum for a) pure PAS and b) MG-PAS

In contrast, the FTIR spectrum of MG-PAS exhibits notable differences, confirming the successful incorporation of malachite green into the PAS lattice. The O–H stretching vibration shifts slightly to 3369 cm⁻¹ and 3343 cm⁻¹, indicating interactions between the PAS lattice and malachite green molecules. The presence of C–H stretching vibrations in MG-PAS at 2980 cm⁻¹, The N–H bending vibration of malachite green appears at 1639 cm⁻¹, which is not observed in pure PAS, further supporting the successful doping process. The sulfate (SO_4^{2-}) stretching vibrations in MG-PAS appear at 1391 cm⁻¹, 1258 cm⁻¹, and 1189 cm⁻¹, showing minor shifts compared to pure PAS, suggesting slight lattice distortions due to doping. Additionally, the C=N stretching vibration of malachite green is observed at 1103 cm⁻¹, confirming its presence within the PAS lattice. The Al–O stretching vibrations at 611 cm⁻¹ and 590 cm⁻¹ in MG-PAS show slight shifts compared to the PAS peak at 596 cm⁻¹, indicating structural modifications due to doping.

These spectral changes confirm that pure PAS contains no carbon-based functional groups, while the incorporation of malachite green alters the vibrational spectrum by introducing additional peaks.

Table no.2 FTIR Peak Assignments for Pure Potash Alum and MO-Doped Potash Alum

Wavenumber (cm⁻¹)	Assignments for Pure PAS	Assignments for MG-Doped PAS
3355	O–H stretching vibration of water (H_2O)	O–H stretching of hydrogen-bonded water molecules, N–H stretching of malachite green

Wavenumber (cm^{-1})	Assignments for Pure PAS	Assignments for MG-Doped PAS
3369, 3343	O–H stretching vibration of water (H_2O)	Asymmetric and symmetric N–H stretching of the NH_2 group in malachite green
2980	O–H stretching vibration of water (H_2O)	C–H stretching vibration of malachite green (aromatic)
2454	O–H stretching of strongly hydrogen-bonded water molecules	O–H stretching of strongly hydrogen-bonded water molecules
1639	–	N–H bending vibration of malachite green
1622	H–O–H bending vibration of water (H_2O)	H–O–H bending vibration of water (H_2O)
1401	Symmetric SO_4^{2-} stretching vibration	Symmetric SO_4^{2-} stretching vibration (slightly shifted)
1391	–	C=C stretching of malachite green (aromatic)
1258	–	C–N stretching of malachite green
1186	S=O asymmetric stretching vibration of sulfate (SO_4^{2-})[1]	S=O asymmetric stretching vibration of sulfate (SO_4^{2-})
1189	–	S=O asymmetric stretching (slightly shifted due to doping)
1103	–	C=N stretching of malachite green
1084	S=O symmetric stretching vibration of sulfate (SO_4^{2-})[1]	S=O symmetric stretching vibration of sulfate (SO_4^{2-})
973	–	Aromatic C–H bending vibration of malachite green
917	S–O stretching vibration of sulfate (SO_4^{2-})	S–O stretching vibration of sulfate (SO_4^{2-})
693	O–S–O bending vibration of sulfate (SO_4^{2-})	O–S–O bending vibration of sulfate (SO_4^{2-})
611	–	Al–O stretching vibration (slightly shifted due to doping)
596	Al–O stretching vibration	–
590	–	Al–O stretching vibration of doped PAS

UV VIS spectral analysis

The UV-Vis transmittance spectra of pure potash alum (PAS), malachite green-doped PAS (MG-PAS), and malachite green dye (MG) are presented in Figure no.4. The pure PAS

crystal exhibits a high transmittance across the visible range, with minimal absorption, demonstrating its excellent optical transparency.

For MG-PAS, the incorporation of malachite green dye results in the appearance of distinct absorption bands at 313 nm, 424 nm, and 607 nm, which correspond to the characteristic electronic transitions of malachite green. The absorption peak at 313 nm corresponds to $\pi \rightarrow \pi$ transitions in MG's phenyl rings, while the 424 nm band originates from $n \rightarrow \pi^*$ transitions in its conjugated chromophore (–N=CH–Ph framework). The peak at 607 nm corresponds to the charge transfer transitions influenced by the molecular interactions between the MG dye and the PAS host lattice[18].

Compared to pure PAS, the MG-doped PAS crystal exhibits a reduction in transmittance, indicating electronic interactions between the MG dye molecules and the PAS lattice. The transmission cut-off wavelength shifts from 216 nm in pure PAS to above 230 nm in MG-PAS, confirming modifications in the optical band gap due to doping. The average transmittance in the visible region remains high, with MG-PAS maintaining reasonable transparency while incorporating the dye molecules.

These results confirm the successful incorporation of malachite green into the PAS matrix, leading to notable changes in its optical absorption characteristics. Such modifications suggest the potential application of MG-PAS crystals in nonlinear optics, photonics, and dye-based optical devices.
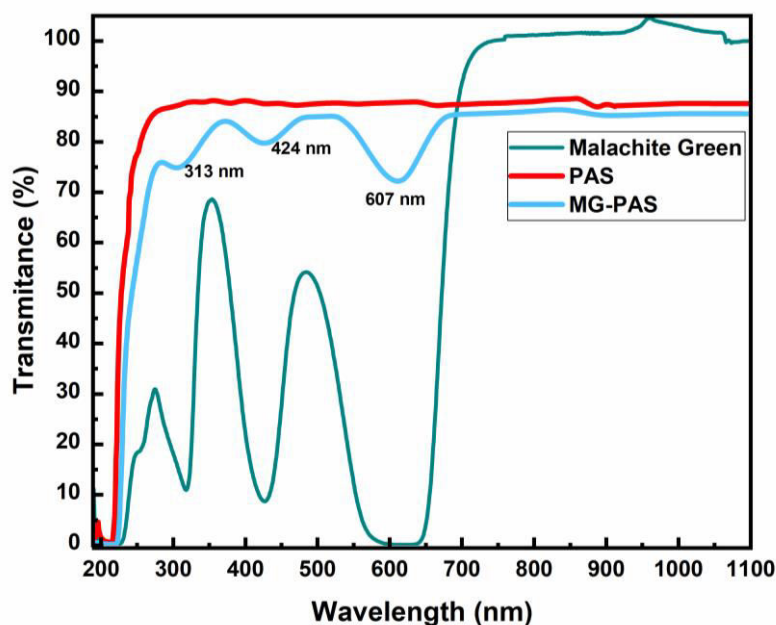

Fig. 4. UV transmission spectra for a) pure PAS and b) MO-PAS

To further analyze the optical properties, the optical absorption coefficient (α) was calculated from transmittance (T) using the relation:

$$\alpha = (2.303 \log (1/T))/d \qquad \qquad \ldots\ldots\ldots(1)$$

where d = 4 mm is the crystal thickness.

For direct band gap materials like potash alum crystals, the absorption coefficient (α) and photon energy (hν) follow the Tauc relation:

$$(\alpha h\nu)^2 = A(h\nu - E_g) \qquad\qquad \text{………(2)}$$

where A is a constant, and Eg is the optical band gap. Tauc plots (Figure 5) were used to determine the band gaps for pure PAS and MO-PAS by extrapolating the linear portion of $(\alpha h\nu)^2$ vs. hν to the x-axis.
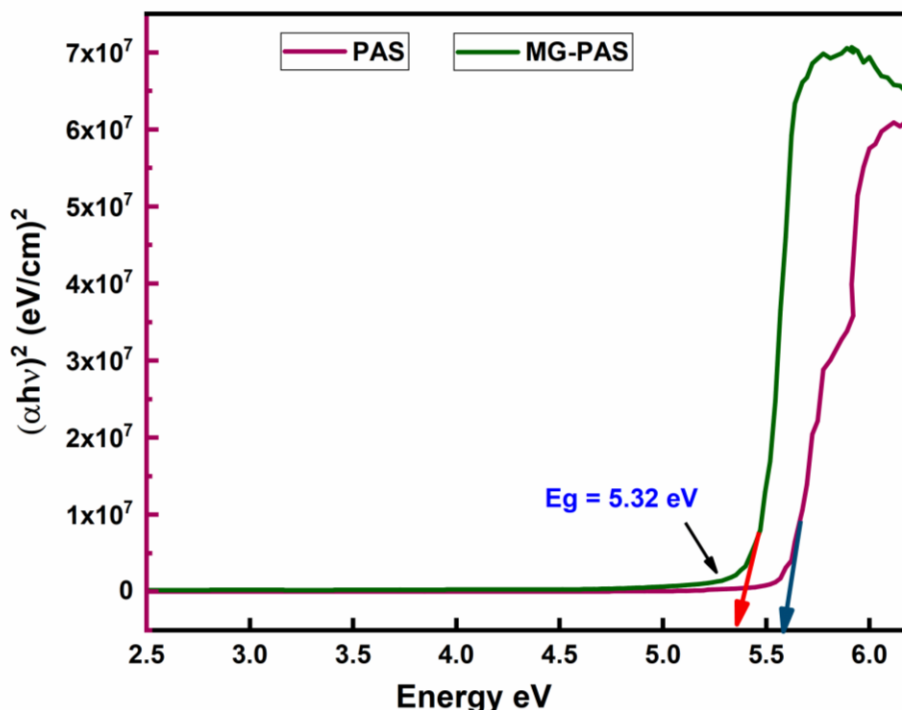

Fig. 5. Tauc's plot for a) pure PAS and b) MG-PAS

The optical band gap of pure PAS (5.60 eV) decreased to 5.32 eV upon malachite green (MG) doping, confirming modified electronic properties. This reduction arises from new defect states introduced by MG, which lower the energy required for electron transitions. Comparable band gap narrowing has been observed in dye-doped crystalline systems, including methyl orange-modified K_2SO_4 and potassium pentaborate octahydrate (MOPPB)[21,14]. The doped crystals also exhibit broad optical transparency across visible and near-infrared wavelengths, making MG-PAS a promising candidate for nonlinear optical (NLO) devices and integrated photonics.

Thermal analysis

The thermogravimetric analysis (TGA) and differential thermal analysis (DTA) of pure PAS and MG-PAS crystals are shown in Figures 6 and 7, respectively.
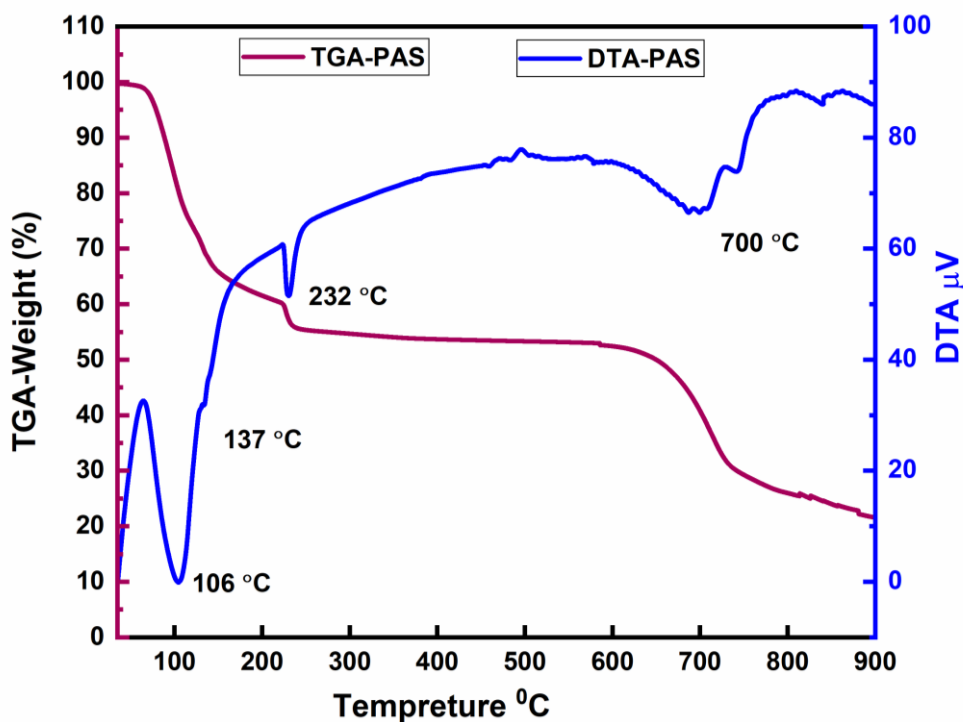
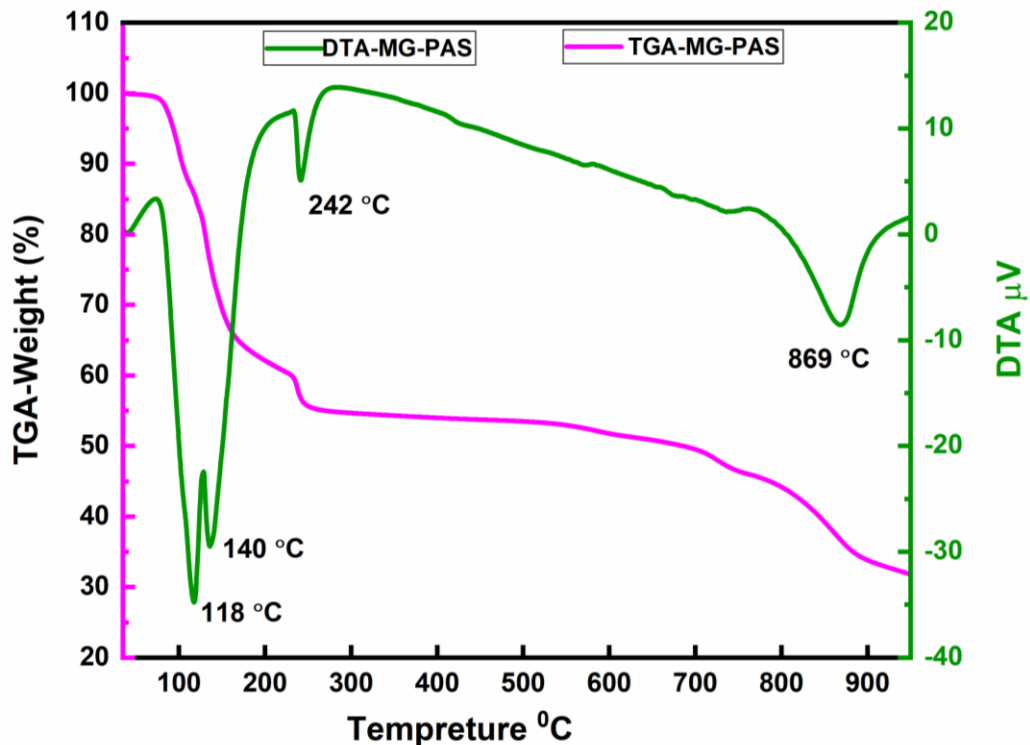Fig. 6. TGA-DTA curve for PAS.

Fig. 7. TGA-DTA curve for MG-PAS.

The thermal behavior of Malachite Green (MG)-doped Potash Alum (PAS) crystals was analyzed using Thermogravimetric Analysis (TGA) and Differential Thermal Analysis (DTA), revealing significant modifications in thermal stability and decomposition patterns due to MG incorporation. The thermal decomposition of PAS (Potash Alum) follows a three-stage degradation process, closely resembling the thermal behavior of reported literature [22-24].In pure PAS, a structural phase transition occurs at approximately 106°C, whereas in MG-doped PAS, this transition shifts to 118°C, indicating enhanced lattice stability. This shift is attributed to the amine ($-N(CH_3)_2$) groups of MG, which likely form hydrogen bonds with sulfate and water molecules in the PAS lattice, reinforcing the crystal structure and increasing the energy required for phase transition.

The dehydration process in pure PAS occurs in two primary steps: the release of loosely bound water around 137°C and the elimination of tightly bound water near 232°C. In MG-doped PAS, these dehydration temperatures increase slightly to 118°C and 242°C, suggesting stronger interactions between water molecules and MG's functional groups. MG's amine ($-N(CH_3)_2$) groups contribute to enhanced hydrogen bonding, making it necessary to supply more thermal energy to disrupt and release water molecules from the crystal structure[18].

Upon further heating, PAS undergoes complete decomposition around 700°C, breaking down into potassium sulfate (K_2SO_4), aluminum oxide (Al_2O_3), and sulfur trioxide (SO_3) gas[24]. In MG-doped PAS, the final decomposition shifts to approximately 869°C, indicating improved thermal stability. This enhancement can be attributed to π-π interactions between the aromatic rings of MG and the PAS matrix, which strengthen intermolecular forces and delay the breakdown of the crystal lattice.

The incorporation of MG into PAS not only enhances its thermal stability but also influences its phase transition mechanisms, making MG-doped PAS more resistant to structural degradation at high temperatures. This increased thermal resilience is of significant scientific interest, as it suggests potential applications in nonlinear optics, dielectric materials, and thermal sensing technologies, where materials must withstand extreme thermal and structural conditions.

Z-Scan Analysis

The third-order nonlinear optical (NLO) properties of MG-PAS crystals were studied using the Z-scan technique with a 632.8 nm He-Ne laser. The beam, adjusted to 5 mm, was focused onto a 1 mm-thick sample using a 200 mm focal length convex lens. The sample was scanned along the Z-axis, and a photodetector with a digital power meter recorded the transmitted intensity. In the closed-aperture setup, a 2 mm-radius aperture was used to determine the nonlinear refractive index (n_2), while in the open-aperture setup, the nonlinear absorption coefficient (β) was measured. The results indicate that MG-PAS crystals exhibit significant NLO properties, making them promising for optical switching and photonic applications.

The open- and closed-aperture Z-scan transmittance curves of pure PAS and MG-PAS crystals are graphically represented in Figures 7a, 7b, 8a, and 8b.
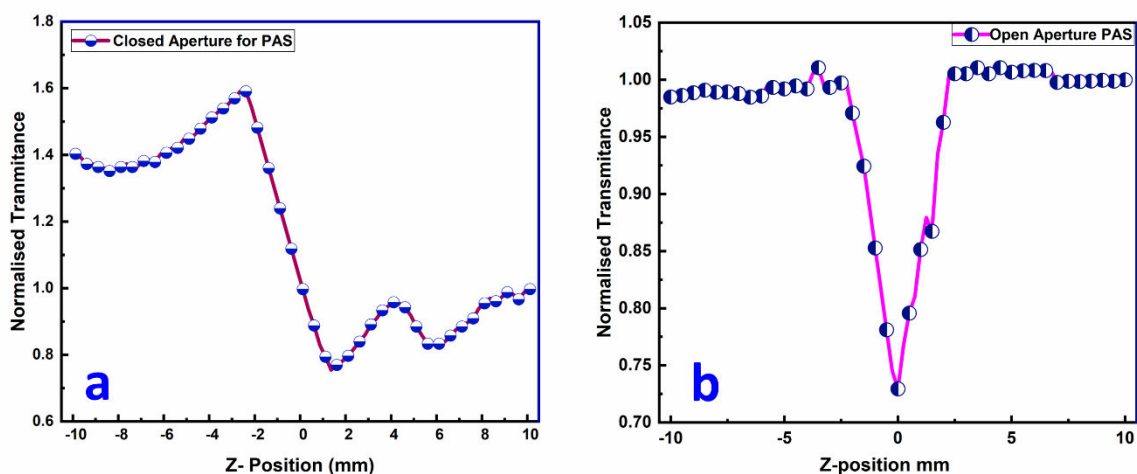
Fig. 7. a and b. Closed and Open aperture Z-scan curves of grown PAS crystal
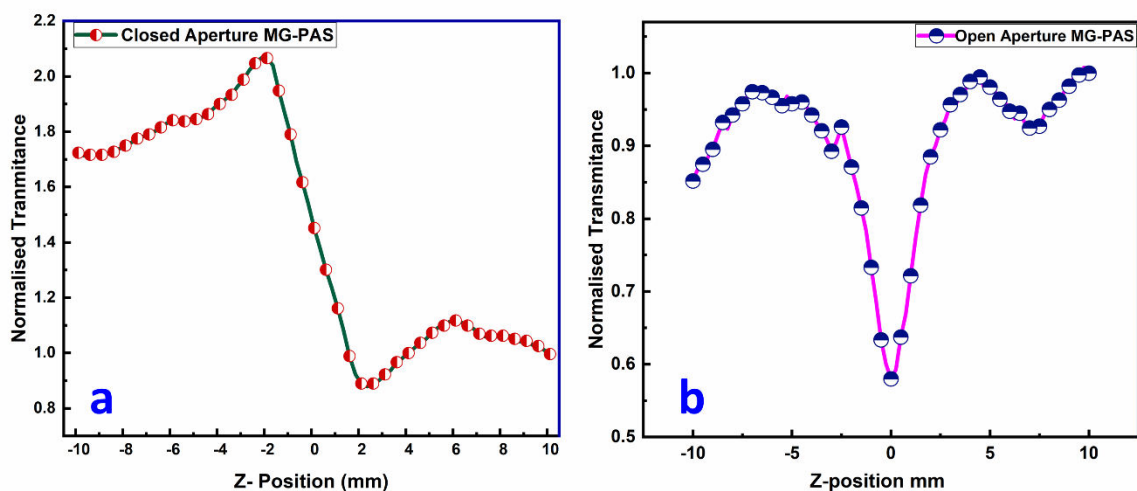

Fig. 8. a and b. Closed and Open aperture Z-scan curves of grown MO-PAS crystal

     The Z-scan analysis of MG-doped PAS (MG-PAS) crystals in the closed-aperture configuration exhibits a pre-focus peak followed by a post-focus valley, confirming a negative nonlinear refractive index (n_2). This self-defocusing behavior arises due to thermal lensing effects, where high-intensity laser irradiation alters the refractive index across the crystal surface[25]. The negative n_2 results from localized thermal accumulation caused by the repetitive exposure to the 632.8 nm He-Ne laser, making MG-PAS suitable for optical limiting and all-optical switching applications[26,27].

     The open-aperture Z-scan data reveal reverse saturable absorption (RSA), characterized by decreased transmittance at the focal point compared to peripheral positions. This suggests a dominant excited-state absorption (ESA) mechanism, where nonlinear

absorption increases due to multi-photon absorption (MPA) under high-intensity light. The incorporation of MG molecules enhances the third-order NLO response due to intramolecular charge transfer (ICT) between donor (–N(CH$_3$)$_2$) and acceptor (–Cl) groups. This charge transfer strengthens the dipole moment variation upon laser excitation, significantly improving the nonlinear refractive index (n$_2$) and RSA.[26]

These findings confirm that MG-PAS crystals exhibit superior nonlinear optical properties, making them highly suitable for 3D fluorescence imaging, optical switching, optical limiting, microfabrication, and frequency up-conversion applications. The essential formulae for computing n$_2$, β, and χ^3 are well-documented in the literature,[28] with the systematically obtained values summarized in Table 3.

Table no. 3 Third-order nlo parameters of PAS, MO-PAS crystals.

NLO parameters	PAS	MG-PAS
Laser beam wavelength (λ)	632.8 nm	632.8 nm
Optical bath length	85 cm	85 cm
Beam radius of the aperture (ωa)	4.5 mm	4.5mm
Aperture radius (ra)	2.0 mm	2.0mm
Sample thickness (L)	1.0 mm	1.0 mm
Effective thickness (Leff)	4.6674 mm	4.5351 mm
Nonlinear refractive index (n2)	3.5928×10^{-10} (m^2 / W)	5.3411×10^{-10} (m^2 / W)
Nonlinear absorption coefficient (β)	1.1538×10^{-3} (m/W)	1.4844×10^{-3} (m/W)
Real part of third-order susceptibility (Re(χ3))	1.9329×10^{-8} esu	2.8734×10^{-8} esu
Imaginary part of third-order susceptibility (Im(χ3))	3.1276×10^{-7} esu	4.0235×10^{-7} esu
Third-order nonlinear optical susceptibility (χ3)	3.1335×10^{-7} esu[29]	4.0338×10^{-7} esu

Malachite Green (MG) enhances the nonlinear optical (NLO) properties of Potash Alum (PAS) through its π-conjugated system, intramolecular charge transfer (ICT), and multi-photon absorption (MPA). The delocalized π-electrons in MG increase polarizability, strengthening both the nonlinear refractive index (n$_2$) and nonlinear absorption coefficient (β). MG doping also reduces the optical band gap (from 5.60 eV in PAS to 5.32 eV in MG-PAS), facilitating stronger electronic transitions and amplifying NLO effects. The Z-scan results confirm a negative nonlinear refractive index (n$_2$) due to thermal lensing and reverse saturable absorption (RSA) from excited-state absorption (ESA)[29]. These enhancements make MG-PAS a promising material for optical switching, limiting, and photonic applications, with χ(3) values outperforming several other NLO crystals (Table 4).

Table no. 4 Third-order nonlinear optical comparison.

Crystal	Third-order susceptibility ($\chi^{(3)}$)	References
MG-PAS	4.0338×10^{-7} esu	Present work
CV-L-PCCM	4.826×10^{-7} esu	[30]
$MgSO_4$-SA	6.32×10^{-10} esu	[31]
KCL-SA	7.848×10^{-10} esu	[32]
KDP	3.72×10^{-14} esu	[33]

Conclusion

Pure PAS and Malachite Green (MG)-doped PAS crystals were successfully grown using the slow evaporation solution technique, and the influence of MG doping on their structural, optical, thermal, and nonlinear optical properties was systematically examined. PXRD analysis confirmed that MG incorporation did not disrupt the cubic structure of PAS but enhanced crystallinity, indicating strong molecular interactions within the PAS matrix. FTIR spectra revealed shifts in vibrational modes due to electrostatic interactions between MG's positively charged cations and the sulfate (SO_4^{2-}) groups in PAS, along with additional hydrogen bonding effects from MG's amine ($-N(CH_3)_2$) groups.

UV-Vis analysis demonstrated a decrease in the optical band gap from 5.60 eV (pure PAS) to 5.32 eV (MG-PAS), suggesting that MG-induced electronic transitions facilitate stronger charge transfer interactions within the PAS matrix. This is attributed to the π-conjugated system of MG, which enhances dipole interactions, leading to increased polarizability. Thermal analysis revealed that MG doping improved lattice stability by shifting the phase transition temperature from 106°C (pure PAS) to 118°C (MG-PAS). This enhancement arises from stronger electrostatic interactions between MG^+ and SO_4^{2-}, as well as π-π stacking effects between MG molecules and the sulfate network, leading to increased thermal resilience.

The nonlinear optical (NLO) properties of MG-PAS exhibited substantial improvements. The nonlinear refractive index (n_2) increased from 3.5928×10^{-10} m²/W (pure PAS) to 5.3411×10^{-10} m²/W (MG-PAS), while the nonlinear absorption coefficient (β) increased from 1.1538×10^{-3} m/W to 1.4844×10^{-3} m/W. The real and imaginary parts of the third-order nonlinear optical susceptibility (χ^3) also exhibited significant enhancement, leading to an overall increase from 3.1335×10^{-7} esu (pure PAS) to 4.0338×10^{-7} esu (MG-PAS). These enhancements arise from intramolecular charge transfer (ICT), multi-photon absorption (MPA), and local field effects induced by MG doping. The self-defocusing nature of MG-PAS, evident from the negative nonlinear refractive index, makes it highly suitable for optical limiting and photonic switching applications.

The incorporation of MG into PAS significantly enhances its crystallinity, optical properties, thermal stability, and nonlinear optical behavior. These findings establish MG-PAS as a promising material for advanced photonic and optoelectronic applications, particularly in nonlinear optics, optical limiting, and thermal sensing technologies.

Acknowledgment

We sincerely thank the SAIF, IIT Madras, for providing the analytical facilities and conducting the Single Crystal X-ray Diffraction (SXRD) analysis crucial for this study. We also declare that this work was conducted without any external funding or financial support.

Conflict of Interest

The authors declare that they have no conflict of interest.

References

1. C. Bhargava, V. K. Banga, and Y. Singh, Fabrication and Failure Prediction of Carbon-alum solid composite electrolyte based humidity sensor using ANN, 25, 773 (2018). DOI: 10.1515/SECM-2016-0272/MACHINEREADABLECITATION/RIS

2. N. Wijayati, L. R. Lestari, L. A. Wulandari, F. W. Mahatmanti, S. K. Rakainsa, E. Cahyono, and R. A. Wahab, Potassium Alum [KAl(SO4)2·12H2O] solid catalyst for effective and selective methoxylation production of alpha-pinene ether products, Heliyon 7, e06058 (2021). DOI: 10.1016/J.HELIYON.2021.E06058

3. A. Alisaac, M. Alsahag, M. Alshareef, R. M. Snari, M. Alhasani, H. M. Abumelha, and N. M. El-Metwaly, Development of smart cotton fabrics immobilized with anthocyanin and potassium alum for colorimetric detection of bacteria, Inorg Chem Commun 145, 110023 (2022). DOI: 10.1016/J.INOCHE.2022.110023

4. C. T. A. Y. Wang, and D. Lu, Study On Oral Ulcer Powder Using Temperature-Dependent X-Ray Diffraction Technique, 1, 104 (2018). DOI: 10.26480/icnmim.01.2018.104.106

5. H. Uzkul, and R. Alkan, Antimicrobial Properties of Silk Fabrics Dyed with Green Walnut Shell (Juglans regia L.), 1, 28 (2018). DOI: 10.34088/KOJOSE.410163

6. P. (2000) H. una educación eficaz para todos: L. educación inclusiva. Monográfico. educar en el 2000. mayo 2002. 15-19 Arnaiz Sánchez, www.congreso.gob.pe/comisiones/2006/discapacidad/tematico/.../inclusion.pdf, and mayo 2002 | educar en el 2000 | 15. Monográfico. HACIA UNA EDUCACIÓN EFICAZ PARA TODOS... Pilar Arnaiz Sánchez. Hacia una educación eficaz para .., Synergistic antibacterial interaction between an alum and antibiotics on some microorganism, Sci J Med Res 2, 47 (2018). DOI: .

7. Y. Shang, J. Xu, H. Sha, Z. Wang, C. He, R. Su, X. Yang, and X. Long, Nonlinear optical inorganic sulfates: The improvement of the phase matching ability driven by the structural modulation, Coord Chem Rev 494, 215345 (2023). DOI: 10.1016/J.CCR.2023.215345

8. Y. Li, C. Yin, X. Yang, X. Kuang, J. Chen, L. He, Q. Ding, S. Zhao, M. Hong, and J. Luo, A Nonlinear Optical Switchable Sulfate of Ultrawide Bandgap, 3, 2298 (2021). DOI: 10.31635/CCSCHEM.020.202000436

9. M. R. Suresh Kumar, H. J. Ravindra, and S. M. Dharmaprakash, Synthesis, crystal growth and characterization of glycine lithium sulphate, J Cryst Growth 306, 361 (2007). DOI: 10.1016/J.JCRYSGRO.2007.05.015

10. A. M. Abdulwahab, K. Mohammad AL-Dhabyani, A. Ahmed Ali Ahmed, N. Mohammed Al-Hada, and A. A. Qaid, The effect of lithium doping on structural, thermal, optical and electrical properties of potash alum single crystals, Inorg Chem Commun 145, (2022). DOI: 10.1016/j.inoche.2022.109985

11. J. Arumugam, N. Suresh, M. Selvapandiyan, S. Sudhakar, and M. Prasath, Effect of NaCl on the properties of sulphamic acid single crystals, Heliyon 5, e01988 (2019). DOI: 10.1016/J.HELIYON.2019.E01988

12. C. P. Sahana, P. R. Deepthi, M. Challa, P. M. Kumar, A. Sukhdev, and J. Shanthi, Exploring the Influence of FeSO4 on the Structural and Thermal Properties of Sulphamic Acid Single Crystals, 47, 275 (2023). DOI: 10.1007/S40995-022-01407-1/METRICS

13. R. Ramesh Babu, R. Ramesh, R. Gopalakrishnan, K. Ramamurthi, and G. Bhagavannarayana, Growth, structural, spectral, mechanical and optical properties of pure and metal ions doped sulphamic acid single crystals, Spectrochim Acta A Mol Biomol Spectrosc 76, 470 (2010). DOI: 10.1016/J.SAA.2010.04.001

14. D. Jini, M. Aravind, S. Ajitha, C. Parvathiraja, M. Muniyappan, P. A. Vivekanand, P. Kamaraj, N. Arumugam, A. I. Almansour, R. Arulnangai, R. S. Kumar, K. Perumal, and G. Gonfa, Synthesis, Growth, and Characterization of Methyl Orange Dye-Doped Potassium Sulphate Single Crystal and Its Multifaceted Activities, 2022, 4020288 (2022). DOI: 10.1155/2022/4020288

15. S. Bhandari, N. Sinha, G. Ray, and B. Kumar, Enhanced optical, dielectric and piezoelectric behavior in dye doped zinc tris-thiourea sulphate (ZTS) single crystals, Chem Phys Lett 591, 10 (2014). DOI: 10.1016/j.cplett.2013.11.007

16. S. Bhandari, N. Sinha, G. Ray, and B. Kumar, Enhanced optical, dielectric and piezoelectric behavior in dye doped zinc tris-thiourea sulphate (ZTS) single crystals, Chem Phys Lett 591, 10 (2014). DOI: 10.1016/J.CPLETT.2013.11.007

17. R. Saini, and D. Joseph, Optical and thermal properties of rhodamine B dye-doped sulphamic acid single crystals, 35, 1 (2024). DOI: 10.1007/S10854-024-12552-1/METRICS

18. G. Durgababu, G. J. Nagaraju, and G. Bhagavannarayana, Effect of malachite green dye doping in tristhiourea zinc (II) sulphate single crystal—a potential nonlinear optical material, 32, 2564 (2021). DOI: 10.1007/S10854-020-05023-W/METRICS

19. V. S. Sukumaran, and A. Ramalingam, Nonlinear studies of malachite green polymer, 124, 3001 (2013). DOI: 10.1016/J.IJLEO.2012.09.010

20. A. M. Abdulwahab, Y. A. A. Al-magdashi, A. Meftah, D. A. Al-Eryani, and A. A. Qaid, Growth, structure, thermal, electrical and optical properties of potassium aluminum sulfate dodecahydrate (potash alum) single crystal, 60, 510 (2019). DOI: 10.1016/J.CJPH.2019.05.034

21. K. Kamatchi, S. Sriram, K. Sangeetha, E. Anuranjani, M. Durairaj, and T. C. Sabari Girisun, Enhanced third-order nonlinear optical properties of methyl orange dye-doped potassium penta borate octa hydrate (MOPPB) single crystals using CW diode laser for optical limiting applications, 32, 15171 (2021). DOI: 10.1007/S10854-021-06067-2/METRICS

22. R. Souza, R. Navarro, A. V. Grillo, and E. Brocchi, Potassium alum thermal decomposition study under non-reductive and reductive conditions, 8, 745 (2019). DOI: 10.1016/J.JMRT.2018.05.017

23. J. Pysiak, and A. Glinka, Thermal decomposition of basic aluminium potassium sulphate. Part I. Stages of decomposition, Thermochim Acta 44, 21 (1981). DOI: 10.1016/0040-6031(81)80267-5

24. R. Wojciechowska, W. Wojciechowski, and J. Kamiński, Thermal decompositions of ammonium and potassium alums, 33, 503 (1988). DOI: 10.1007/BF01913929/METRICS

25. W. Ji, B. Gu, and H.-T. Wang, Z-scan technique for investigation of the noninstantaneous optical Kerr nonlinearity, 34, 2769 (2009). DOI: 10.1364/OL.34.002769

26. S. P. Ramteke, S. Kalainathan, M. Anis, G. G. Muley, M. I. Baig, and H. Algarni, Novel report on luminescence, linear and laser induced optical traits of potassium aluminium sulphate crystal for photonic device applications, Optik (Stuttg) 201, 163509 (2020). DOI: 10.1016/J.IJLEO.2019.163509

27. S. Shettigar, G. Umesh, K. Chandrasekharan, and B. Kalluraya, Third order nonlinear optical properties and two photon absorption in newly synthesized phenyl sydnone doped polymer, Synth Met 157, 142 (2007). DOI: 10.1016/J.SYNTHMET.2007.01.003

28. P. Karuppasamy, V. Sivasubramani, M. S. Pandian, and P. Ramasamy, Growth and characterization of semi-organic third order nonlinear optical (NLO) potassium 3,5-dinitrobenzoate (KDNB) single crystals, RSC Adv 6, 109105 (2016). DOI: 10.1039/C6RA21590D

29. S. P. Ramteke, S. Kalainathan, M. Anis, G. G. Muley, M. I. Baig, and H. Algarni, Novel report on luminescence, linear and laser induced optical traits of potassium aluminium sulphate crystal for photonic device applications, Optik (Stuttg) 201, (2020). DOI: 10.1016/j.ijleo.2019.163509

30. M. Akilan, R. Ragu, J. P. Angelena, and S. J. Das, Enhancement in mechanical, optical, SHG, photoacoustic and Z-scan studies on pure and crystal violet dye doped L-proline cadmium chloride single crystal for nonlinear optical applications, 30, 3655 (2019). DOI: 10.1007/S10854-018-00645-7/METRICS

31. J. Arumugam, M. Selvapandiyan, S. Chandran, M. Srinivasan, and P. Ramasamy, Effect of MgSO4 on sulphamic acid single crystals and their structural, optical, mechanical, thermal and third order nonlinear optical studies, Mater Chem Phys 242, 122479 (2020). DOI: 10.1016/J.MATCHEMPHYS.2019.122479

32. J. Arumugam, M. Selvapandiyan, S. Chandran, M. Srinivasan, and P. Ramasamy, Crystal growth, optical, thermal, laser damage threshold, photoconductivity and third-order nonlinear optical studies of KCl doped sulphamic acid single crystals, 31, 6084 (2020). DOI: 10.1007/S10854-020-03161-9/METRICS

33. R. A. Ganeev, I. A. Kulagin, A. I. Ryasnyansky, R. I. Tugushev, and T. Usmanov, Characterization of nonlinear optical parameters of KDP, LiNbO3 and BBO crystals, Opt Commun 229, 403 (2004). DOI: 10.1016/J.OPTCOM.2003.10.046